Journal of *Marine Science and Engineering*

MDPI

Article

A Study on the Spatial Morphological Evolution and Driving Factors of Coral Islands and Reefs in the South China Sea Based on Multi-Source Satellite Imagery

Fengyu Li [1,2], Wenzhou Wu [1,*], Peng Zhang [1], Bingyue Zhang [1] and Fenzhen Su [1]

[1] State Key Laboratory of Geographic Information Science and Technology, Institute of Geographic Sciences and Natural Resources Research, Chinese Academy of Sciences, Beijing 100101, China; lifengyu24@mails.ucas.ac.cn (F.L.); zhangpeng2112@igsnrr.ac.cn (P.Z.); zhangbingyue402x@igsnrr.ac.cn (B.Z.); sufz@lreis.ac.cn (F.S.)

[2] College of Resources and Environment, University of Chinese Academy of Sciences, Beijing 101408, China

* Correspondence: wuwz@lreis.ac.cn

Abstract: The spatial morphology of coral islands and reefs is a fundamental physical and ecological attribute that reflects the developmental and evolutionary processes of coral islands and reefs. The spatial morphology of coral islands and reefs in the South China Sea is highly dynamic. Understanding the evolutionary trends of the spatial morphology of these coral islands and reefs is crucial for their sustainable development and utilization. This study proposes a set of stability evaluation indicators for reef spatial morphology and conducts a systematic analysis of the spatial morphological changes in coral islands and reefs in the South China Sea over the past 15 years, based on 96 satellite images. Additionally, the driving factors behind these changes are explored and discussed. The results indicate the following: (1) The spatial morphology of the Xisha islands and reefs exhibits more significant changes compared to the Nansha islands and reefs. Although both the Xisha and Nansha islands and reefs areas are increasing, the area change in Xisha is 1.3 times greater than that in Nansha. (2) The spatial morphology of the Xisha islands and reefs is shifting in all directions, while the Nansha islands and reefs show a more pronounced northwestward movement. (3) Both the Xisha and Nansha islands and reefs show an overall growth trend, with the growth rate of the Xisha islands and reefs being faster than that of the Nansha islands and reefs. The average growth rate of the Xisha islands and reefs is 1.77 times that of the Nansha islands and reefs. This research provides significant scientific evidence for the protection and resource management of coral islands and reefs in the South China Sea.

Keywords: South China Sea; shoreline change; island evolution; coral reefs and islands

check for updates

Academic Editor: Tom Spencer

Received: 24 March 2025
Revised: 15 April 2025
Accepted: 17 April 2025
Published: 20 April 2025

Citation: Li, F.; Wu, W.; Zhang, P.; Zhang, B.; Su, F. A Study on the Spatial Morphological Evolution and Driving Factors of Coral Islands and Reefs in the South China Sea Based on Multi-Source Satellite Imagery. *J. Mar. Sci. Eng.* **2025**, *13*, 820. https://doi.org/10.3390/jmse13040820

Copyright: © 2025 by the authors. Licensee MDPI, Basel, Switzerland. This article is an open access article distributed under the terms and conditions of the Creative Commons Attribution (CC BY) license (https://creativecommons.org/licenses/by/4.0/).

1. Introduction

Coral islands and reefs, often referred to as the "tropical rainforests" of the ocean, are among the most biodiverse ecosystems on Earth. They are also one of the most productive ecological units in the ocean, characterized by the highest primary productivity and the most active calcification processes [1,2]. Coral reef islands are mostly composed of coral debris and biogenic sediments, with a low altitude and weak erosion resistance. They are considered one of the landforms most vulnerable to anthropogenic climate change and sea-level rise [3,4]. The South China Sea is one of the world's typical coral island and reef distribution zones, with extensive coverage, large reef areas, and a variety of coral shoals and islands. These coral islands and reefs not only offer crucial support to regional

ecosystems but also play an important role in regulating both global and regional climate change. As a result, coral islands and reefs in the South China Sea have become a focal point of research for scholars both domestically and internationally [5].

According to the latest Assessment Report (AR6) of the Intergovernmental Panel on Climate Change (IPCC), the global mean sea level is projected to rise by 40–63 cm by the end of this century, with significant impacts on coral islands and reefs [6]. The spatial morphology of coral islands and reefs not only reflects their developmental and evolutionary processes but is also one of their most fundamental physical and ecological attributes [7]. Changes in spatial morphology are strongly driven by natural environmental factors and external dynamic processes, directly affecting coral islands and reefs' stability and ecosystem functions [8]. Coral islands and reefs in the South China Sea are primarily formed through the long-term accumulation of shallow-water reef-building corals and associated biogenic materials. Due to their extremely low elevation and sparse vegetation, they are highly susceptible to external environmental conditions [9]. Under the influence of the complex oceanic dynamic system of the South China Sea, the spatial morphology of coral islands and reefs is continuously shaped by monsoons, typhoons, and hydrodynamic forces such as waves, tides, and ocean currents, placing them in a state of dynamic evolution [10]. This characteristic results in morphological instability for some coral islands and reefs, with their spatial distribution patterns potentially changing over time [11]. Furthermore, increasing human activities, such as land reclamation and fishing, have intensified disturbances to the natural evolution of coral islands and reefs, further exacerbating their spatial instability [5]. Against this backdrop, the stability and future development of the spatial morphology of coral islands and reefs in the South China Sea have become key topics of interest in the international marine science community [12]. In-depth research on the evolution of coral island and reef spatial morphology not only enhances our understanding of their natural dynamic processes but also provides a scientific basis for developing coral island and reef conservation policies, optimizing resource management strategies, and addressing global climate change [13].

Remote-sensing technology, with its advantages of wide coverage, high temporal resolution, multi-temporal monitoring, and long-term data accumulation, has become an essential tool for monitoring and analyzing the spatial morphological dynamics of coral islands and reefs [14]. In particular, high-resolution remote sensing, with its superior spatial resolution and positional accuracy, enables rapid monitoring of coral island and reef morphological changes and provides a scientific basis for analyzing long-term trends [15]. Early studies on the spatial morphology of coral islands and reefs in the South China Sea primarily used area as the main characteristic indicator to estimate their coverage [16]. However, these estimations were mostly based on traditional nautical charts, lacking high-precision field survey data and clear remote-sensing imagery, which resulted in significant uncertainties in coral island and reef area statistics, with no consensus reached to date [17]. In recent years, international scholars have employed optical remote sensing and hyperspectral remote-sensing techniques for detailed monitoring of coral island reef spatial morphology. For example, Zhou, S. et al. used remote-sensing technology to analyze the spatial morphological evolution of coral islands and reefs in the Nansha islands, focusing on shoreline dynamics from 2009 to 2017 and exploring influencing factors [18]. Additionally, some studies have focused on changes in reef coastlines and island morphology, analyzing parameters such as perimeter, shape indices, and dynamic

evolution patterns [19]. Other research has concentrated on the evolution of coral island and reef ecosystems, using remote-sensing monitoring to assess spatial distribution changes in shoreline biotic communities and their ecological responses [20]. Most of these studies, however, remain limited to single-time analyses or localized changes within specific periods, lacking comprehensive examinations of long-term time series and multi-temporal imagery. This limitation restricts a deeper understanding of the long-term evolutionary trends of coral islands and reefs.

The spatial morphology of coral island and reef shorelines is inherently dynamic. In coral island and reef ecological research and management, the analysis of historical shoreline change rates is widely recognized as a fundamental approach for characterizing shoreline evolution processes [21]. Through the quantification of shoreline change rates, the extent of spatial transformation can be systematically assessed, and the impacts of anthropogenic activities on coral island and reef ecosystems can be indirectly evaluated [22]. The Digital Shoreline Analysis System (DSAS), developed by the United States Geological Survey (USGS), has been extensively applied as an analytical framework for modeling and computing the spatiotemporal rates of shoreline change over a given period. DSAS was utilized by Nirsobha Bhuyan et al. to analyze the migration of riverbanks within the floodplain of the Brahmaputra River in Assam, India, over a 30-year period (1990–2020), and projections for riverbank positions in 2030 and 2040 were made [23]. The Digital Shoreline Analysis System (DSAS) was utilized by Nassar K, Mahmod W E, Fath H, et al. to analyze shoreline changes at Worthing Beach, Barbados, using historical aerial photographs from 1973 to 2004, with projections extending to 2023. It was observed that Hurricane Allen (1980) and Hurricane Ivan (2004) resulted in shoreline accretion and erosion, respectively, with these changes primarily attributed to variations in the height of the coral rubble reef. Emphasis was placed on the necessity of thoroughly understanding the underlying causes of accretion and erosion before implementing engineering interventions [24]. However, previous studies have been predominantly concentrated on the morphological evolution of continental shorelines, while relatively little attention has been given to the dynamics of coral island and reef shorelines.

The spatial morphology of coral islands and reefs in the South China Sea exhibits significant spatial heterogeneity. Existing studies have primarily focused on localized regions or single-temporal data analyses, and comprehensive, high-precision assessments of coral island and reef morphology in the South China Sea remain relatively limited. In particular, systematic investigations incorporating long-term time series analyses are still scarce. To address that research gap, this study proposes a reef spatial morphological stability assessment framework and conducts a systematic analysis of the spatiotemporal evolution of coral islands and reefs in the South China Sea over the past 15 years, utilizing multi-source satellite remote-sensing imagery. The analysis encompasses key morphological indicators, including area change rate, length change rate, centroid shift rate, and endpoint rate, facilitating a comparative assessment of coral island and reef morphological evolution as well as an exploration of its driving factors. This study aims to provide a data foundation for understanding ecological and environmental changes in the coral island and reef systems of the South China Sea, offer scientific insights for predicting future reef morphological trends, and serve as a theoretical basis for policy formulation, ecological conservation, and the sustainable development and utilization of island resources.

2. Data and Methods

A workflow for exploring changes in SEA islands' coastline was established (Figure 1).

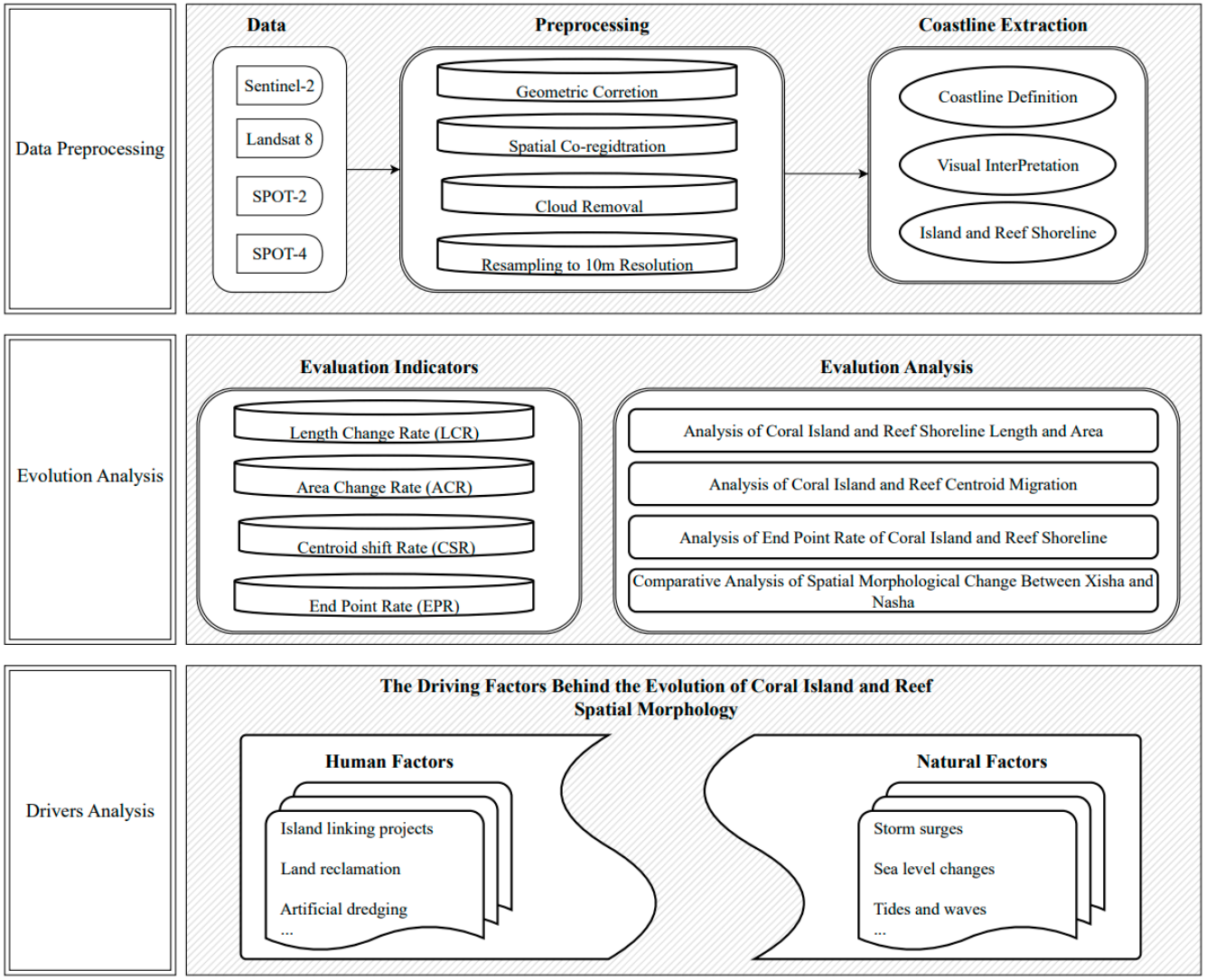


Figure 1. Workflow of study.

2.1. Overview of the Study Area

The South China Sea, located to the south of the Chinese mainland and in the western Pacific Ocean, is a semi-enclosed sea extending in a northeast–southwest direction. The region contains nearly 300 islands and reefs, which are categorized into four major archipelagos: the Dongsha (Pratas) islands, the Xisha (Paracel) islands, the Zhongsha (Macclesfield) islands, and the Nansha (Spratly) islands [25,26]. The Dongsha islands consist of Dongsha Island and several nearby coral shoals and submerged reefs [27]. The Xisha islands comprise more than 30 sand islands, reef islands, sand cays, and reef flats [28]. The Zhongsha islands include over 20 submerged shoals and reefs. The Nansha islands contain more than 230 sand islands, reef islands, sand cays, and reef flats [29]. However, most of these features do not possess natural conditions suitable for human habitation. Among them, a total of 86 geographic features remain exposed either permanently or at low tide. Based on factors such as habitation status and exposed land area, 24 representative coral islands and reefs were selected for this study, including 12 islands and reefs from the Xisha islands and 12 from the Nansha islands (Figure 2), all of which maintained an exposed land area of over 10,000 m^2 between 2007 and 2022 (Table 1).

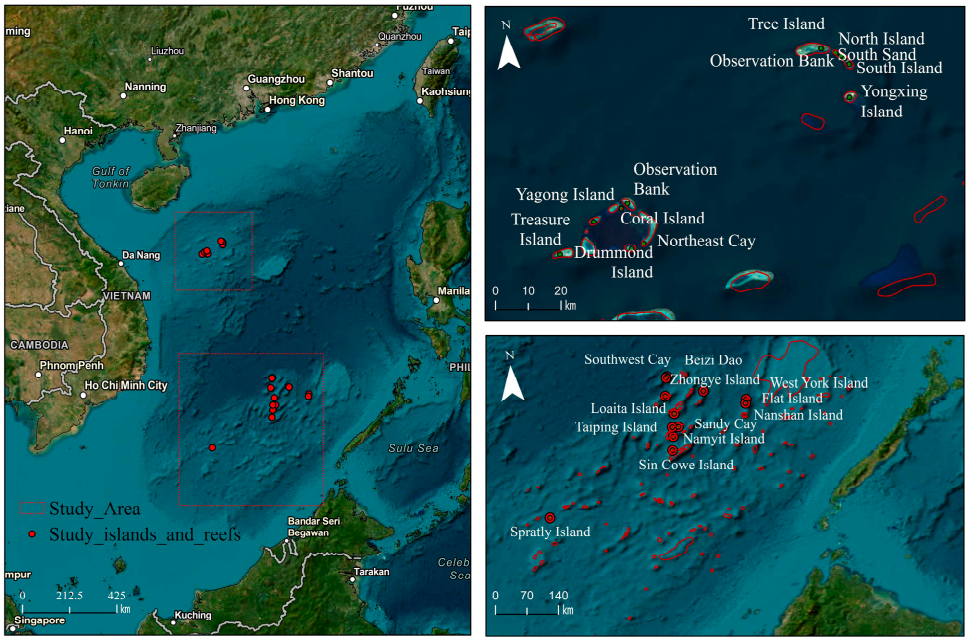


Figure 2. Study area.

Table 1. Location information of selected coral islands and reefs (WGS84).

Xisha Islands				Nansha Islands			
Name	**Type**	**Lat**	**Lon**	**Name**	**Type**	**Lat**	**Lon**
Yongxing Island	Inhabited	16.8344	112.3397	Namit Island	Inhabited	10.1794	114.3664
Duncan Island	Inhabited	16.4497	111.7075	Taiping Island	Inhabited	10.3764	114.3653
North Island	Inhabited	16.9636	112.3103	Zhonghe Island	Inhabited	11.0533	114.2847
Treasure Island	Inhabited	16.4478	111.5081	Sandy Cay	Inhabited	10.3747	114.48
Coral Island	Inhabited	16.5342	111.6072	Spratly Island	Inhabited	8.6453	111.92
Tree Island	Inhabited	16.9794	112.2708	West York Island	Inhabited	11.0817	115.0242
Drummond Island	Inhabited	16.4628	111.7414	Southwest Cay	Inhabited	11.4289	114.3317
Yagong Island	Inhabited	16.5664	111.6864	Northeast Cay	Inhabited	11.4525	114.3542
Observation Bank	Inhabited	16.5794	111.7042	Sin Cowe Island	Inhabited	9.8853	114.3297
Middle Island	Uninhabited	16.9556	112.3241	Loaita Island	Inhabited	10.6678	114.4242
South Island	Uninhabited	16.9472	112.334	Nanshan Island	Inhabited	10.7325	115.8031
South Sand	Uninhabited	16.9297	112.3458	Flat Island	Inhabited	10.8147	115.8225

2.2. Data Sources and Processing

Multi-source satellite remote-sensing imagery was utilized, integrating data from different satellites based on their temporal coverage and spatial resolution. The selected remote-sensing data sources included Sentinel-2 imagery from the European Space Agency (ESA), Landsat 8 imagery from the National Aeronautics and Space Administration (NASA), and SPOT-2 and SPOT-4 imagery from the French National Centre for Space Studies (CNES). Given the significant influence of monsoons and typhoons on the spatial stability of coral islands and reefs in the South China Sea, imagery selection was conducted with careful consideration of seasonal conditions. Since the South China Sea monsoon prevails from July to September in the Northern Hemisphere, imagery from September to November of 2007, 2012, 2017, and 2022 was selected, corresponding to periods near spring high tide. This approach ensured that each reef was represented by four images at different time points, with each image containing red, green, blue, and near-infrared bands, resulting in a total of 96 scenes (Table 2). To ensure spatial consistency and accuracy, standardized preprocessing of the imagery was conducted using ENVI 5.6 (Exelis Visual Information Solutions, America). The preprocessing steps included geometric correction, spatial co-registration (with Sentinel-2 imagery as the reference), cloud removal, and image enhancement. Finally, all images were resampled to a uniform 10 m resolution, ensuring consistency in spatial resolution across different data sources and time periods. Through these processes, a reliable dataset was established to support subsequent analyses.

Table 2. Remote-sensing imagery.

Satellite	Agency	Sensor	Spectral Bands	Acquisition Period	Spatial Resolution (m)
Sentinel-2	ESA	MSI	Red, Green, Blue, NIR	October–November 2022	10
Landsat 8	NASA	OLI	Red, Green, Blue, NIR	September–November 2017	30 and 15
SPOT4	CNES	HRVIR	Red, Green, Blue, NIR	September–November 2012	20
SPOT2	CNES	HRV	Red, Green, Blue, NIR	September–November 2007	20

2.3. Definition of Coral Island and Reef Shoreline

The shoreline of coral islands and reefs refers to the boundary between land and ocean. Due to tidal forces, this boundary is dynamic, with distinct high-tide and low-tide lines marking the extremes of water level. The area between these two lines is known as the intertidal zone. The width of the intertidal zone varies depending on the region and time of year. Unlike some definitions that consider the high-water mark during spring tides as the shoreline, the shoreline in this study is defined as the land–sea boundary recorded in satellite remote-sensing imagery. Although it is not possible to definitively determine whether these recorded boundaries represent the high-tide or low-tide lines, it is certain that they lie within the intertidal zone, which reflects the spatial morphology of the coral islands and reefs to some extent. In this study, a human–machine interactive visual interpretation method was used to extract the instantaneous waterline, which represents the boundary of the spatial morphology of coral island and reef sandbars.

2.4. Evaluation Indicators

The evaluation indicators selected in this study include the length change rate (LCR), measured in meters per year (m/year), area change rate (ACR), measured in square meters per year (m^2/year), centroid shift rate (CSR), measured in meters per year (m/yr), and the endpoint rate (EPR), also measured in meters per year (m/year).

The length change rate (LCR) is an indicator that describes the rate of change in the coastline over a certain time period, used to quantify the extent of coastline change. It reflects the rate of coastline expansion or retreat. Its calculation formula is

$$LCR = \frac{L_t - L_0}{T} \tag{1}$$

where LCR is the coastline length change rate, with unit of m/year, L_t is the coastline length at time t, L_0 is the coastline length at the reference time (usually the initial time), T is the time interval between the two time points, $LCR > 0$ indicates an increase in coastline length, typically corresponding to sediment deposition, and $LCR < 0$ indicates a decrease in coastline length, usually corresponding to erosion.

The area change rate (ACR) is an indicator used to quantify the rate of change in the area of islands or reefs over a specific time period. It reflects the extent of island or reef area expansion or contraction. Its calculation formula is

$$ACR = \frac{A_t - A_0}{T} \tag{2}$$

where ACR is the area change rate, with the unit of m^2/year, A_t is the island or reef area at time t, A_0 is the area at the reference time (usually the initial time), T is the time interval between the two time points, $ACR > 0$ indicates that the island or reef area has expanded, with larger values indicating a faster sedimentation rate, $ACR < 0$ indicates that the island or reef area has shrunk, with larger values indicating a faster erosion rate, and $ACR = 0$ indicates no significant change in island or reef area during the time period.

The centroid shift rate (CSR) is commonly used to monitor changes in island morphology and spatial migration, especially when islands or reefs are influenced by natural factors (such as ocean erosion, sedimentation, etc.) or human activities (such as land reclamation, construction projects, etc.). The calculation method is generally based on the spatial coordinates of the island's centroid at different times and is calculated as follows:

$$CSR = \frac{D}{T_{final} - T_{initial}} \tag{3}$$

where D is the migration distance of the centroid position (calculated as the difference in central coordinates), and $T_{final} - T_{initial}$ is the time interval between the two measurements. The larger the CSR value, the more significant the island's change, with the unit of m/year.

The endpoint rate (EPR) is the average movement rate between the coastline positions of two different years, calculated by dividing the distance between the initial and final coastline positions by the time interval. It is used to analyze the spatial characteristics of coastline change:

$$EPR = \frac{D_{final} - D_{initial}}{T_{final} - T_{initial}} \tag{4}$$

where D_{final} is the distance from the endpoint position to the baseline along the tangent, $D_{initial}$ is the distance from the starting point position to the baseline along the tangent, and $T_{final} - T_{initial}$ is the time interval between the two measurements, with the unit of m/year.

3. Results and Analysis

Considering the geographical location and environmental differences between the Nansha islands and the Xisha islands, this study analyzes the spatial morphological changes and variations in coral islands and reefs in these two regions separately.

3.1. Changes in Coral Island and Reef Size and Morphology

3.1.1. Changes in the Size and Morphology of Xisha Coral Islands and Reefs

By extracting shoreline data from 2007, 2012, 2017, and 2022 for the 12 coral islands and reefs in the Xisha islands, the corresponding shoreline lengths and reef areas were quantified, as presented in Table 3. To further elucidate the spatiotemporal variations in the size and morphology of the Xisha coral islands and reefs, a comprehensive analysis was conducted based on changes in shoreline dynamics and reef area expansion or contraction.

Table 3. Shoreline length and area of Xisha coral islands and reefs (2007–2022).

Coral Islands and Reefs	Length (Unit: Meter)				Area (Unit: Square Meter)			
	2007	2012	2017	2022	2007	2012	2017	2022
North Island	3443.72	3176.17	3626.85	3573.32	380,943.74	328,444.81	342,124.73	343,776.30
Duncan Island	7487.07	7438.28	7315.27	6988.63	548,012.55	716,563.75	716,552.40	722,518.23
Drummond Island	2174.66	2241.87	2115.14	2006.74	271,044.00	253,351.89	206,018.43	210,091.97
Treasure Island	3689.97	3614.09	3055.85	4057.79	376,083.54	374,227.54	347,981.85	401,704.35
South Island	1952.71	2059.23	2047.41	1941.20	112,380.98	111,059.30	109,008.52	126,216.17
South Sand	1564.42	1223.76	1358.65	1275.16	51,745.55	51,228.65	51,884.26	55,007.59
Coral Island	2891.09	2651.55	2711.27	3071.53	302,510.26	290,925.90	297,598.15	312,723.88
Yagong Island	534.90	579.65	507.07	528.92	15,876.24	15,645.53	11,896.64	11,749.42
Yongxing Island	12,610.98	15,657.49	13,575.48	11,715.33	2,261,673.24	2,407,303.65	3,210,077.26	3,244,285.09
Observation Bank	826.29	1020.95	719.59	588.27	11,395.40	11,975.77	11,735.68	12,717.30
Middle Island	1442.58	1510.20	1463.40	1500.62	110,410.36	112,900.39	112,392.40	116,499.11
Tree Island	1850.06	1679.47	3644.23	3651.06	170,963.27	162,389.35	282,357.48	277,935.73

In terms of the shoreline length of the coral islands and reefs, as shown in Figure 3, from 2007 to 2022, Yongxing Island experienced the most significant change in shoreline length. From 2012 to 2022, the shoreline length continuously decreased, showing a decline of 7.79% compared to 2007, although it still maintained a relatively long shoreline. Additionally, Treasure Island and Tree Island saw substantial changes in shoreline length in certain years. Other reefs, such as North Island, Coral Island, and Yagong Island, exhibited relatively small changes in shoreline length, remaining generally stable or showing slight fluctuations. Specifically, Yagong Island's length remained at a relatively low level, with no significant upward or downward trend.

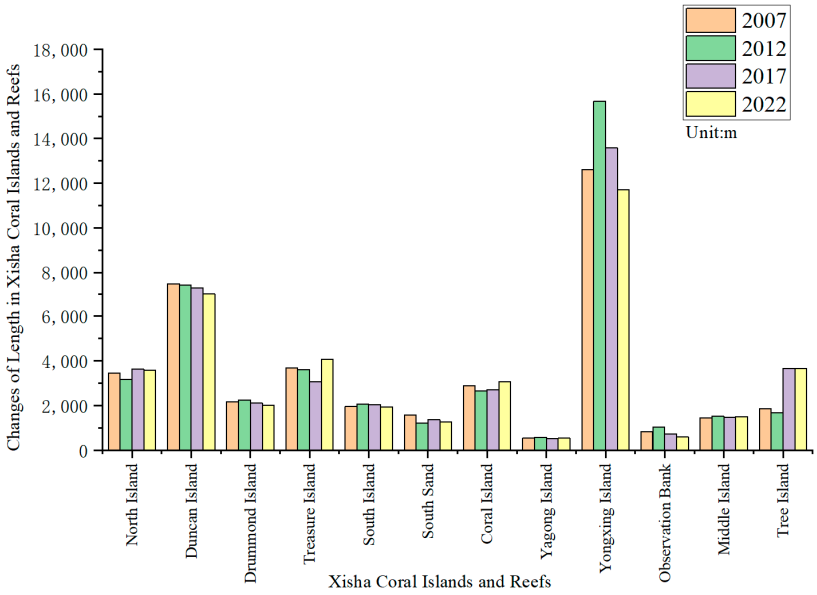


Figure 3. Changes in the shoreline length of Xisha coral islands and reefs from 2007 to 2022.

The analysis of changes in the length of the coastline of islands and reefs, as illustrated in Figure 4, revealed significant variations in the rate of these changes for Tree Island, Treasure Island, and Yongxing Island from 2007 to 2022. The rate of shoreline changes at Tree Island initially increased and subsequently decreased, peaking from 2012 to 2017 at an rate of 393 m/year. The shoreline changes at Treasure Island exhibited a pattern of initial decrease followed by a rapid increase, indicating periods of erosion followed by accretion. In contrast, Yongxing Island experienced a sharp decline in shoreline length, followed by a minor recovery, reflecting a significant reduction in its coastline.

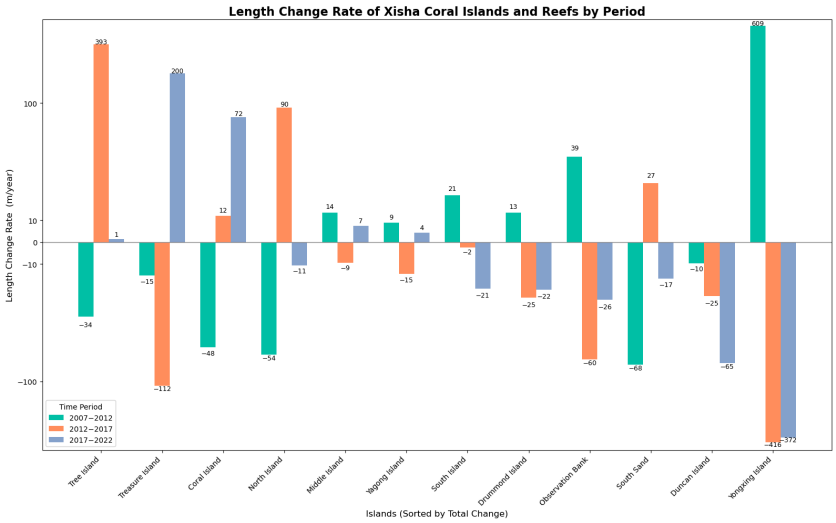


Figure 4. Changes in the *LCR* of Xisha coral islands and reefs from 2007 to 2022.

Regarding the changes in the area of the islands and reefs, as shown in Figure 5, the area fluctuations are more pronounced, especially for Drummond Island and Treasure Island. Yongxing Island, on the other hand, exhibits a strong growth trend, with its area increasing by approximately 43% over 15 years. Treasure Island also experienced significant area growth (about 6.91%). Overall, between 2012 and 2017, the area of most islands decreased, but from 2017 to 2022, many islands saw area expansion, particularly Treasure Island and Yongxing Island.

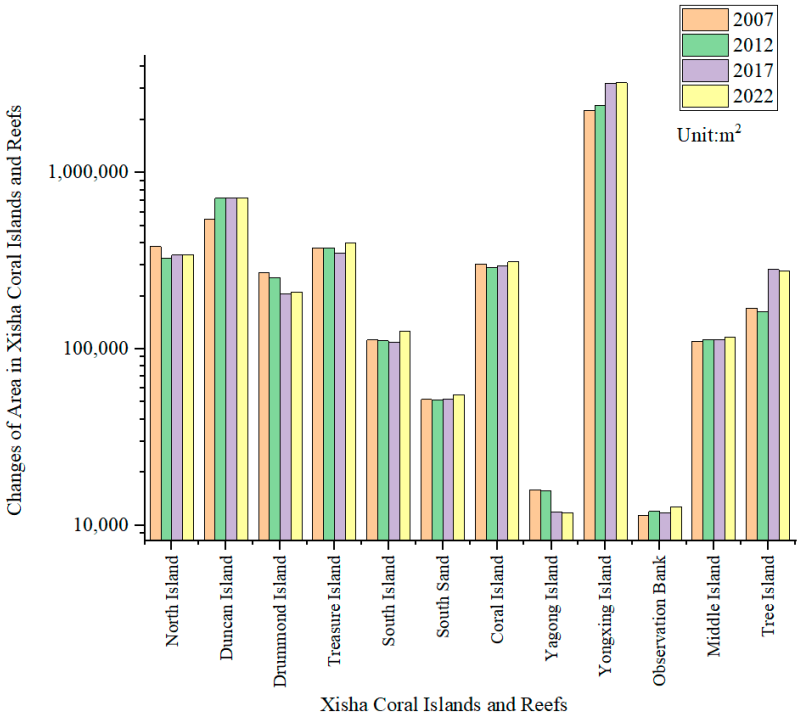


Figure 5. Changes in the area of Xisha coral islands and reefs from 2007 to 2022.

Regarding the rate of changes in the area of the islands and reefs, as shown in Figure 6, from 2007 to 2012, a few islands and reefs exhibited a significant deviation in *ACR* compared to others. Between 2012 and 2017, the differences in *ACR* among the islands and reefs were the largest, while from 2017 to 2022, the *ACR* values of the islands and reefs became more similar. Yongxing Island showed the greatest variation in area change rate, with a sharp increase followed by a sharp decrease. Duncan Island and Tree Island also experienced substantial fluctuations in area change rate. Overall, from 2012 to 2017, the Xisha islands and reefs experienced the largest changes in area, with most islands showing an expansion trend, particularly Yongxing Island, whose area continued to grow with rate, first sharply increasing and then steadily growing.

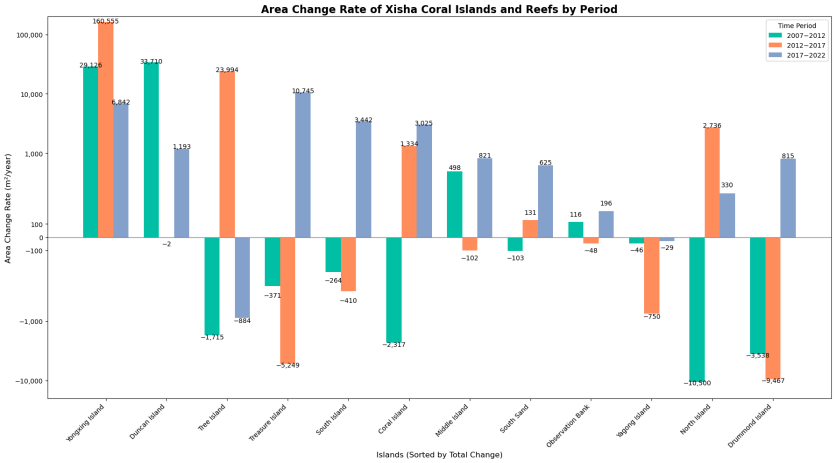


Figure 6. *ACR* changes in the Xisha coral islands and reefs from 2007 to 2022.

3.1.2. Changes in Size and Morphology of the Nansha Coral Islands and Reefs

By extracting the shoreline data of 12 Nansha coral islands and reefs from 2007, 2012, 2017, and 2022, the shoreline length and island area of each Nansha coral island and reef were obtained, as shown in Table 4. The following is a further analysis of the changes in

size and morphology of the Nansha coral islands and reefs based on the shoreline and area of the coral islands and reefs.

Table 4. Shoreline length and area of Nansha coral islands and reefs from 2007 to 2022.

Coral Islands and Reefs	Length (Unit: Meter)				Area (Unit: Square Meter)			
	2007	2012	2017	2022	2007	2012	2017	2022
Northeast Cay	1777.06	2031.90	1789.54	2014.18	141,196.07	177,678.44	158,089.32	161,366.15
Sandy Cay	888.15	939.62	1144.54	4932.12	41,076.63	39,944.21	62,575.76	175,027.53
Flat Island	566.70	702.03	497.47	544.98	8370.82	14,051.38	11,081.37	15,417.96
Namyit Island	1853.83	1963.43	1740.39	6379.42	89,127.57	91,511.22	88,524.34	442,746.63
Sin Cowe Island	931.54	1000.69	2787.61	2597.57	47,004.38	52,086.82	129,770.05	140,706.75
Nanshan Island	1013.63	1162.26	1012.46	1002.40	70,873.79	85,228.50	70,326.66	70,469.34
Spratly Island	1844.27	1812.49	4680.51	4655.88	163,089.90	161,781.80	362,458.93	357,011.63
Loaita Island	1330.62	1160.95	1170.16	1193.80	83,222.42	78,172.69	73,891.34	72,630.61
Southwest Cay	1546.57	2751.07	2743.43	2684.03	144,869.22	185,117.93	179,053.44	187,909.43
Taiping Island	3054.13	3056.29	4623.34	4847.43	426,229.06	410,821.79	457,825.92	489,645.52
West York Island	1820.32	1813.27	1829.87	1833.50	193,821.90	192,662.33	192,697.30	190,819.26
Zhongye Island	3389.78	3470.21	3306.48	4282.87	385,961.45	391,124.31	386,766.58	428,494.01

Regarding the shoreline length of the Nansha islands and reefs, as shown in Figure 7, Sandy Cay and Namyit Island showed significant growth in shoreline length over these years, particularly Sandy Cay, which experienced an extremely notable increase of 455.2%. The shoreline length of Nanshan Island remained almost stable, with a slight decrease of about 1.1%. Flat Island also saw a decline in shoreline length (about 3.9%). Other islands, such as Northeast Cay, Sin Cowe Island, Spratly Island, Taiping Island, etc., exhibited relatively steady growth in shoreline length, typically ranging between 20% and 80%. Overall, the majority of the islands showed an increasing trend in shoreline length, especially Sandy Cay and Namyit Island, which demonstrated a strong expansion trend.

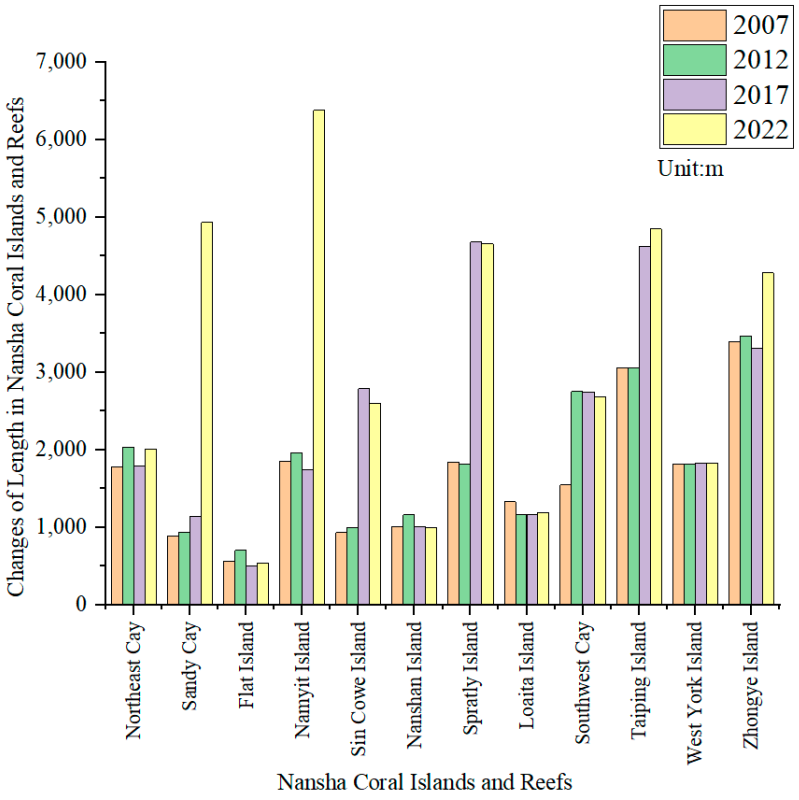


Figure 7. Changes in shoreline length of Nansha coral islands and reefs from 2007 to 2022.

Regarding the rate of changes in shoreline length of the Nansha islands and reefs, as shown in Figure 8, Namyit Island exhibited the most significant shoreline growth, particularly between 2017 and 2022, showing a strong expansion trend (928 m/year). Sandy Cay, Sin Cowe Island, and Spratly Island also demonstrated a strong growth trend, with the intensity of growth noticeably increasing between 2017 and 2022. Other islands, such as Northeast Cay, Flat Island, and Taiping Island, exhibited a stable growth trend with small variations. Overall, the growth rate of Namyit Island between 2017 and 2022 was particularly remarkable, while the shoreline changes in other islands were relatively stable, with only a few islands showing more significant growth.

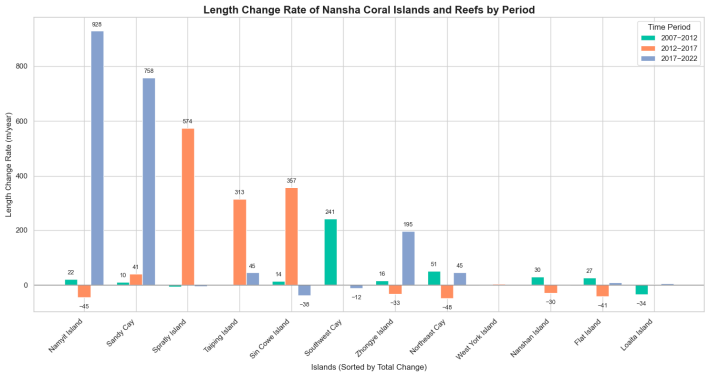


Figure 8. Changes in the *LCR* of Nansha coral islands and reefs from 2007 to 2022.

Regarding the changes in area of the Nansha islands and reefs, as shown in Figure 9, Sandy Cay, Namyit Island, and Sin Cowe Island experienced significant area growth from 2007 to 2022, particularly Namyit Island, which saw an area increase of about 396%. The area changes in these islands reflect their strong expansion during this period. Northeast Cay, Spratly Island, Southwest Cay, Taiping Island, and Zhongye Island exhibited a relatively stable growth trend, with a moderate overall area increase of about 10–30%. Nanshan Island and Loaita Island experienced a decrease in area, particularly Loaita Island, which saw a 12.7% decrease in area over the 15 years, while Nanshan Island showed minimal change. Overall, the area of most islands showed an increasing trend from 2007 to 2022, especially Sandy Cay and Namyit Island, which demonstrated significant expansion.

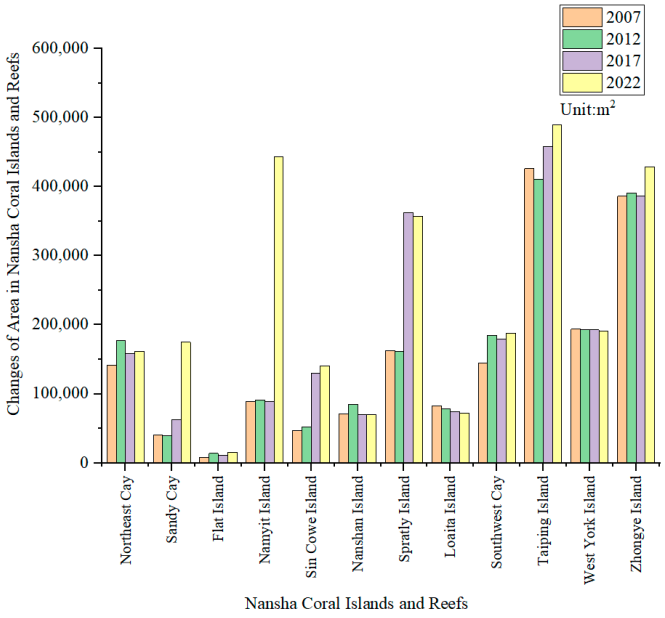


Figure 9. Changes in area of Nansha coral islands and reefs from 2007 to 2022.

Regarding the rate of area changes in the Nansha islands and reefs, as shown in Figure 10, Namyit Island exhibited a very significant area increase between 2017 and 2022, with a growth rate of 70,844 m^2/year, far exceeding that of other islands. Other islands, such as Northeast Cay, Flat Island, Sin Cowe Island, and Spratly Island, showed a more stable growth trend, typically ranging from 8049 m^2/year to 22,490 m^2/year. Islands like West York Island and Zhongye Island exhibited relatively stable changes, with a small overall variation. Overall, most islands showed steady growth during different periods, while Namyit Island demonstrated significant area expansion between 2017 and 2022.

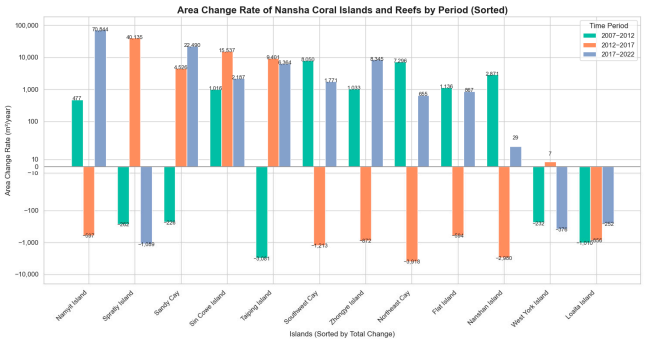


Figure 10. Changes in *ACR* of Nansha coral islands and reefs from 2007 to 2022.

3.2. Analysis of Coral Island and Reef Centroid Migration

In addition to changes in size and shape, the location changes in coral islands and reefs are also very significant. The movement of the location is typically analyzed using the centroid method, where the centroid refers to an imaginary point that represents the concentration of an object's mass and is the average position of the object's mass distribution. This study calculates the centroid position of each island and reef for each period based on the shoreline range at different times, and thus it obtains the location migration trajectory of each island and reef, which facilitates the analysis of the planar location movement of each island and reef.

3.2.1. Analysis of Xisha Coral Island and Reef Centroid Migration

Figure 11 shows that the center migration rate of Yongxing Island significantly increased to 4.34 m/year between 2017 and 2022, with considerable fluctuations, ultimately reaching a rate of 10.39 m/year. The migration rates of Observation Bank and Duncan Island were also quite notable, especially Observation Bank, which exhibited a very high rate between 2012 and 2017 (27.40 m/year). The migration rates of Middle Island, South Island, and South Sand were relatively stable, with small variations and lower overall rates. The migration rates of islands such as Coral Island and Tree Island significantly increased during the final period, particularly Coral Island, which saw a rapid increase in migration rate from 2017 to 2022, reaching 3.91 m/year.

As shown in Figure 12, the centroid positions of Duncan Island, Yongxing Island, Yagong Island, and Observation Bank tend to migrate northward; the centroids of South Island, Middle Island, and Drummond Island are shifting southward; the centroids of Coral Island, Treasure Island, and Tree Island are moving westward; the centroid of North Island is migrating southeastward; and the centroid of South Sand, despite a significant migration in 2012, returned to a position near that of 2007 in 2017 and 2022. Overall, the centroids of the Xisha islands and reefs have shifted in various directions, without a consistent direction.

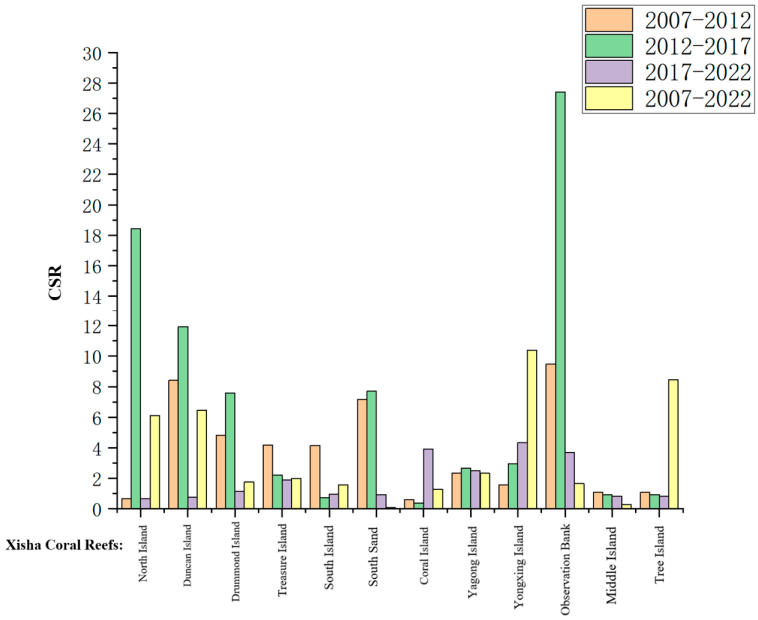


Figure 11. Changes in *CSR* of Xisha coral islands and reefs.

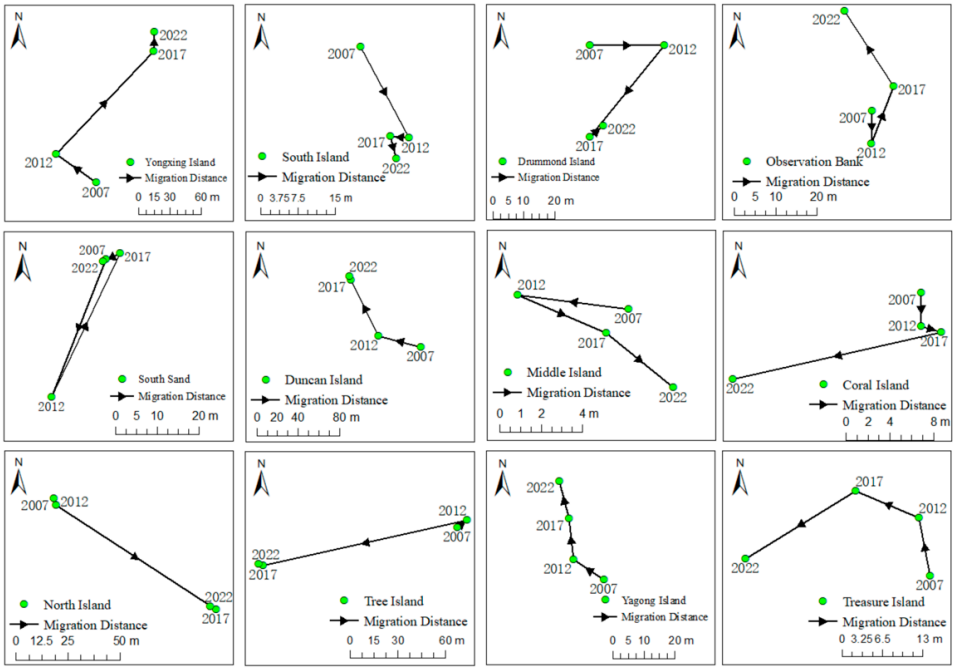


Figure 12. Migration trajectories of Xisha coral islands and reef centroid.

3.2.2. Analysis of Nansha Coral Island and Reef Centroid Migration

Figure 13 shows that the centroid migration rates of Namyit Island and Sandy Cay exhibit significant variations, particularly Namyit Island, which demonstrated a sharp change of 61.09 m/year between 2017 and 2022, showing intense fluctuations in centroid movement. The changes in Spratly Island were also notable, with a migration rate of 17.93 m/year from 2012 to 2017, followed by a sharp decline. The migration rates of Nanshan Island and West York Island showed smaller changes, with overall stability, indicating relatively stable centroid migration. Zhongye Island and Southwest Cay exhibited some fluctuations over different periods, but the changes were relatively smooth, with a lower overall rate.

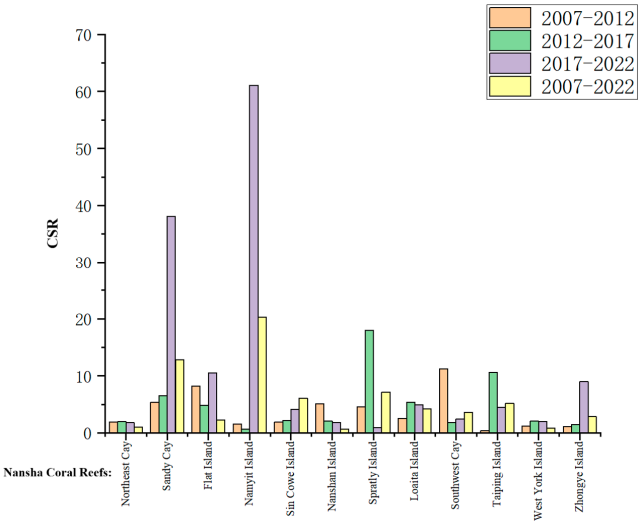


Figure 13. Changes in *CSR* of Nansha coral islands and reefs.

The centroids of Northeast Cay, Namyit Island, and Spratly Island are migrating northward, while the centroids of Sin Cowe Island and Loaita Island are shifting southward (Figure 14). The centroids of Sandy Cay, Southwest Cay, Taiping Island, West York Island, and Zhongye Island are migrating westward. Flat Island and Nanshan Island, on the other hand, migrated northward between 2007 and 2012 but shifted southward between 2012 and 2022. Overall, the migration directions of the centroids of the Nansha coral islands and reefs exhibit a consistent trend, migrating predominantly in the northwest direction.

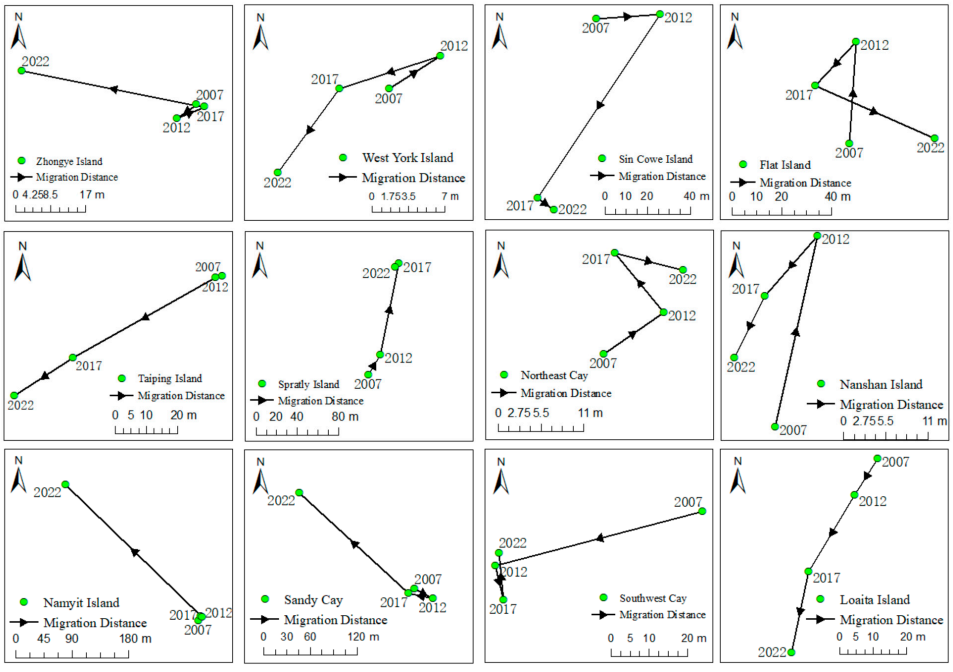


Figure 14. Migration trajectories of Nansha coral island and reef centroid.

3.3. Analysis of Spatial Morphological Change Rate

The ArcGIS-based DSAS 5.0 (U.S. Geological Survey, Reston, VA, USA, Woods Hole, Falmouth, MA, USA) was used in this study, with the shoreline position from the earliest time point, 2007, being set as the baseline. Perpendicular fault planes to the baseline were created at a distance of 40 m, with intervals of 20 m and a smoothing distance of 5 m. These fault planes intersected each shoreline at an endpoint, with each endpoint corresponding to

a specific time point. All the endpoints were extracted by DSAS, and the change in position over time was calculated along the perpendicular line from the baseline to the endpoints of subsequent shoreline positions. Finally, the change rate of each endpoint was calculated based on the change distance and the difference in years. The endpoint change rate in all directions was first calculated for each island and reef, and then the average rate, erosion proportion, maximum erosion rate, average erosion rate, expansion proportion, maximum expansion rate, and average expansion rate were computed for the spatial morphological change rate analysis of the islands and reefs.

3.3.1. Analysis of Spatial Morphological Change Rate of Xisha Coral Islands and Reefs

The *EPR* data of the Xisha coral islands and reefs are shown in Figure 15. It can be observed that the average rate of North Island, Drummond Island, Coral Island, and Yagong Island is below 0, indicating an erosion state, with Drummond Island having the highest erosion rate at −2.73 m/year. Islands with more than 60% of their area in erosion include North Island, Drummond Island, and Yagong Island; those with erosion between 40% and 60% include South Sand, Coral Island, Yongxing Island, and Observation Bank. Among them, Drummond Island has the largest proportion of eroded area, with 89.38%. The maximum erosion rate of Drummond Island is −12.49 m/year, and its average erosion rate is the largest, at −3.15 m/year. At the same time, the proportion of growing coastline for North Island and Drummond Island is less than 20%, while the proportion of growing coastline for Duncan Island, Treasure Island, South Island, Middle Island, and Tree Island exceeds 60%. Yongxing Island has the highest growth rate, reaching 17.61 m/year, and also the highest average growth rate, at around 2.63 m/year.

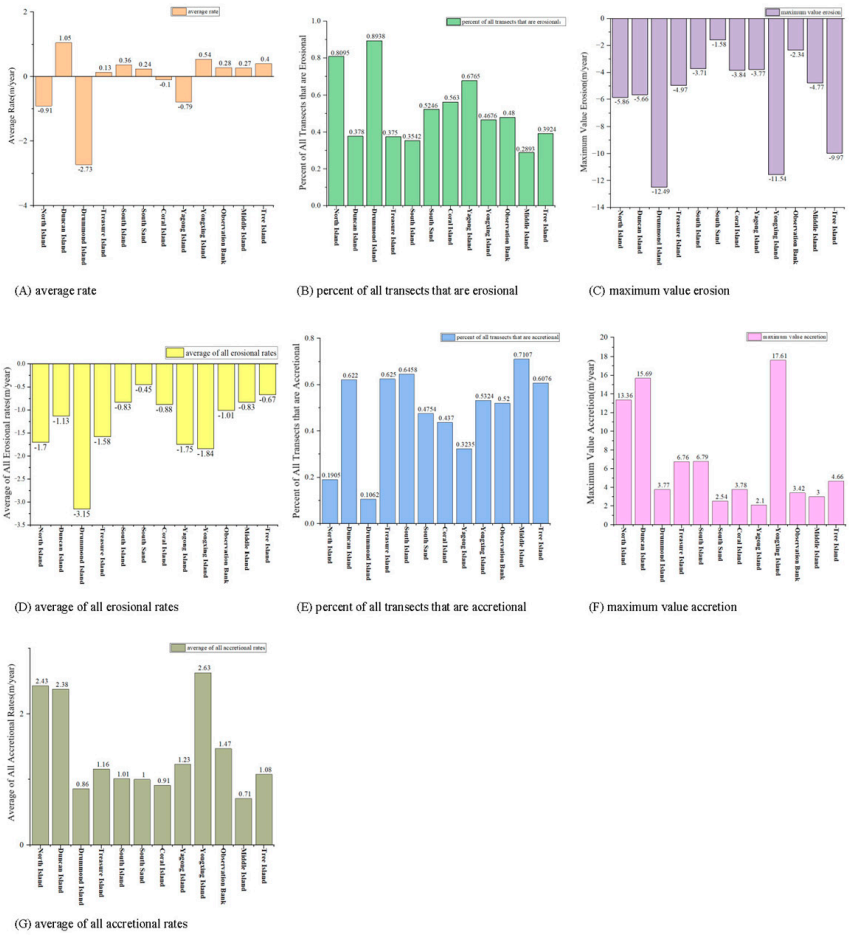


Figure 15. *EPR* of Xisha islands and reefs.

North Island, Drummond Island, Coral Island, and Yagong Island are in an erosion state, with Drummond Island being the most severe, where 89.38% of the coastline area is eroded, and the maximum erosion rate reaches −12.49 m/year. The remaining eight islands and reefs are in a sediment accumulation state, with Duncan Island having the highest average growth rate and 62.2% of its coastline area in the growth zone.

3.3.2. Analysis of Spatial Morphological Change Rate of Nansha Coral Islands and Reefs

The *EPR* data of the Nansha coral islands and reefs are shown in Figure 16. It can be observed that Southwest Cay, West York Island, and Zhongye Island have an average rate below 0, indicating an erosion state. Sandy Cay and Namyit Island have the highest average *EPR*s, at 2.85 m/year and 3.76 m/year, respectively. Additionally, only Spratly Island has more than 60% of its area in an erosion state. The maximum erosion rate of Namyit Island is the highest, at −17.58 m/year. Among them, Loaita Island has the most severe erosion, with an average erosion rate of −2.95 m/year. Meanwhile, Sandy Cay has the highest proportion of growing coastline, at 97.92%. The maximum growth rate of Namyit Island is 27.79 m/year, and its average growth rate is the highest, at around 6.46 m/year.

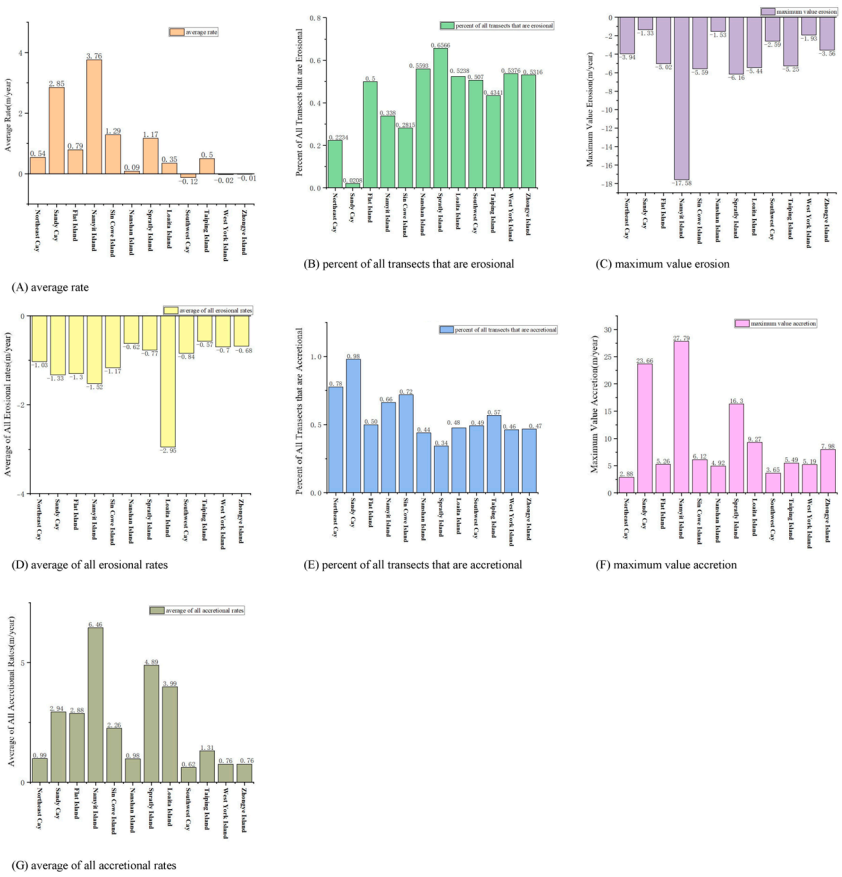


Figure 16. *EPR* of Nansha islands and reefs.

Southwest Cay, West York Island, and Zhongye Island are in an erosion state, but with relatively small erosion rates. Seven islands have more than 50% of their area in an erosion state. Namyit Island shows significant variation, with one part having an erosion rate of −17.58 m/year, while another part exhibits a sediment accumulation growth rate of 27.79 m/year. Although 65.66% of Spratly Island is eroded, the overall trend is sediment accumulation. Overall, compared to the Xisha islands and reefs, the *EPR* changes in

the Nansha islands and reefs are relatively small, with only a few islands showing more noticeable changes, such as Namyit Island.

3.4. Comparative Analysis of Spatial Morphological Changes Between Xisha and Nansha Coral Islands and Reefs

To investigate the patterns of change in the Xisha and Nansha islands and reefs, a comparative analysis was conducted on the area, centroid migration distance, and *EPR* of 12 islands and reefs from both the Xisha and Nansha archipelagos over a 15-year period, as shown in Table 5. The *EPR* and area changes in the Xisha islands and reefs are greater than those of the Nansha islands and reefs, indicating that the morphological changes in the Xisha islands and reefs are more pronounced in comparison. It is noteworthy that the standard deviation of area change in the Xisha islands and reefs is significantly higher than that of the Nansha islands and reefs, being 2.67 times greater, suggesting that the area changes in the Xisha islands and reefs are far more substantial. While the mean, standard deviation, maximum, and minimum values of centroid migration distance for the Xisha islands and reefs are all lower than those for the Nansha islands and reefs, Figure 17 reveals that the directional differences in morphological changes in the Xisha islands and reefs are not as pronounced as those of the Nansha islands and reefs, with the latter showing a more distinct trend of change toward the northwest direction.

Table 5. Comparison of morphological changes between Xisha and Nansha islands and reefs.

Statistic	Archipelago	Total N	Mean	Standard Deviation	Sum	Minimum	Median	Maximum
Centroid Shift Distance Unit: m	Xisha	12	52.86	51.21	634.32	0.98	28.02	155.92
	Nansha	12	83.96	86.20	1007.50	10.47	58.94	304.57
EPR Unit: m/year	Xisha	12	171.55	589.72	2058.62	0.98	1.255	2044.17
	Nansha	12	96.81	404.39	1742.58	0.98	1.475	1717.16
Area Change Unit: m^2	Xisha	12	101,848.83	284,294.72	1,222,186.01	−60,952.03	8151.18	982,611.85
	Nansha	12	78,116.80	106,348.15	937,401.62	−10,591.81	42,786.38	353,619.06

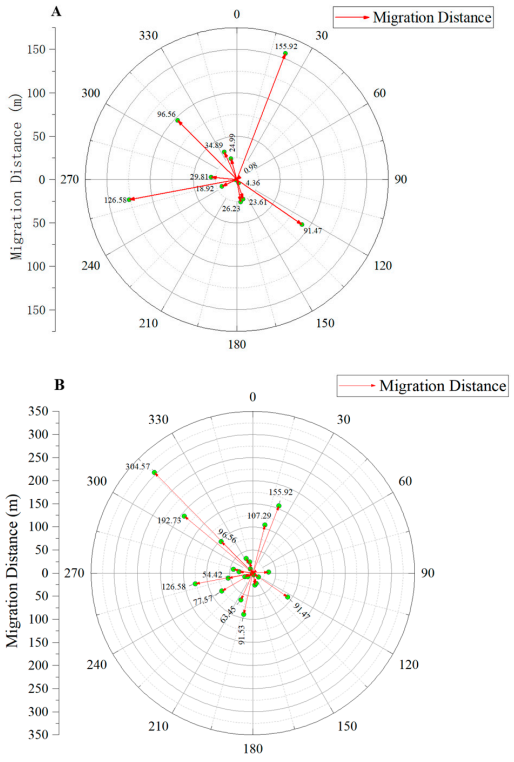


Figure 17. Migration directions of Xisha and Nansha islands and reefs.

4. The Driving Factors Behind the Evolution of Coral Island and Reef Spatial Morphology

According to relevant studies, the factors influencing island and reef morphological changes can primarily be categorized into natural and human factors [30–32]. Human factors mainly include island-linking projects, land reclamation, and the construction and expansion of docks, as well as breakwaters, artificial dredging, and other activities [33]. Natural factors include river sediment discharge into the sea, climate change, storm surges, sea-level changes, tides, and waves [34].

4.1. Human Factors

Based on remote-sensing images and relevant data, there are various human factors influencing the Xisha and Nansha islands and reefs, with land reclamation being the most significant human factor affecting the morphological changes in the islands and reefs (Figure 18). Yongxing Island, located in the Xisha archipelago, is the most densely populated and heavily developed island, and it has also undergone both island-linking projects and land reclamation processes. It was first connected to Rocky Island, and then from the autumn and winter of 2013 to 2014, land reclamation increased its area by 2.2 times, expanding from the original 2.13 square kilometers to 3.16 square kilometers. In the Nansha archipelago, many islands and reefs have also undergone significant changes in spatial morphology due to human intervention. For example, surrounding countries like Vietnam and the Philippines have continuously expanded and upgraded facilities on the Nansha islands, causing major changes in their morphology. In 2008, Vietnam built a harbor basin on Southwest Cay and continued to expand it in 2009. As of now, its area has increased from 1.18 square kilometers in 2007 to 7.45 square kilometers, a growth of approximately 6.31 times. Namyit Island has also undergone island and reef expansion, the construction of lighthouses, and the upgrading of various facilities, resulting in an increase in its area from 0.16 square kilometers in 2007 to approximately 2.13 square kilometers today. In addition, islands such as Spratly Island and Sin Cowe Island have also experienced significant changes in spatial morphology due to human interventions, including land expansion and the construction of facilities.



Figure 18. Satellite images of island and reef changes under human intervention.

4.2. Natural Factors

Although human activities can have a significant impact on the morphology of islands and reefs, the natural factors influencing island and reef morphology should not be overlooked (Figure 19). Sediment brought by waves and tides can deposit around islands and reefs, promoting their expansion or morphological reshaping; the effects of strong waves and tidal currents can also exacerbate erosion around the islands or alter sediment distribution. Additionally, typhoons are an important natural factor affecting the morphological changes in islands and reefs. The South China Sea, located in the monsoon zone of the northwestern Pacific, is one of the regions where typhoons are most frequently generated and occur. After formation in the northwestern Pacific, typhoons often move westward and enter the South China Sea, significantly impacting the islands and reefs in the region. Typhoons trigger storm surges and heavy rainfall, which may lead to flooding disasters in coastal areas. Additionally, strong winds and large waves can damage the South China Sea's island and reef ecosystems (such as coral islands and reefs), altering the local coastal morphology. For example, Yagong Island in the Xisha archipelago shows completely different morphologies in 2012, 2017, and 2022. The island is small, with an area of less than 20,000 m^2, making it vulnerable to factors such as waves, tides, and typhoons, which cause significant morphological changes. The shoreline length increased by 8.37%, decreased by 12.52%, and increased by 4.31%, while the area decreased by 1.45%, 23.96%, and 1.24%, respectively.



Figure 19. Satellite images of Yagong Island changes.

5. Discussion

The spatial morphological evolution of coral islands and reefs in the South China Sea, as revealed by this study, highlights complex interactions between natural dynamics and anthropogenic interventions. The observed differences between the Xisha and Nansha archipelagos underscore the importance of regional environmental heterogeneity and human activity rate in shaping reef stability. Below, we contextualize these findings, discuss their implications, and address limitations and future directions.

5.1. Key Findings

The pronounced morphological changes in the Xisha islands, particularly the rapid expansion of Yongxing Island (1.77 times faster growth rate compared to Nansha), align with documented large-scale land reclamation projects in the region. These findings corroborate previous studies emphasizing human activities as dominant drivers of reef modification in densely populated or strategically important areas [31,33]. Conversely, the northwestward centroid migration trend in the Nansha islands likely reflects natural hydrodynamic processes, such as monsoon-driven sediment transport and typhoon impacts [34], which are less mitigated by human stabilization efforts compared to Xisha. The divergent patterns between the two archipelagos highlight the need for region-specific management strategies.

This study's use of multi-source satellite imagery and stability evaluation indicators (e.g., *CSR*, *EPR*) addresses a critical gap in long-term, high-resolution analyses of coral reef

systems. Earlier works relying on single-timepoint or low-resolution data [17] often underestimated the dynamic nature of reef morphology, particularly in regions with episodic natural disturbances (e.g., typhoons) or abrupt anthropogenic changes. Our findings demonstrate that integrating multi-temporal remote-sensing data significantly enhances the accuracy of trend detection, as seen in the fluctuating erosion–accretion patterns of islands like Treasure Island and Namyit Island.

5.2. Mechanistic Insights

Human activities, particularly land reclamation and infrastructural development, emerged as primary drivers of rapid morphological changes. For instance, Yongxing Island's area expansion (43% over 15 years) and Southwest Cay's sixfold growth directly correlate with documented construction activities (Figure 18). These interventions often override natural sediment dynamics, creating artificial stability in some areas while exacerbating erosion in others (e.g., Drummond Island's 89% shoreline erosion). Such outcomes align with global observations of human-altered reef systems, where short-term gains in land area come at the cost of long-term ecological resilience [5,11].

Natural factors, including typhoons and monsoonal hydrodynamics, played a dual role. While typhoon-induced wave energy contributed to episodic erosion (e.g., Yagong Island's fluctuating shoreline), monsoonal currents facilitated sediment redistribution, driving the northwestward migration of Nansha reefs. This aligns with models predicting increased reef mobility under climate change scenarios (IPCC AR6), where rising sea levels and storm intensity may further destabilize low-lying islands.

5.3. Limitations and Future Directions

While this study advances our understanding of reef dynamics, several limitations warrant attention. First, the 15-year timeframe may not fully capture decadal-scale cyclical patterns (e.g., El Niño/La Niña effects). Second, the resolution of older SPOT imagery (20 m) might obscure fine-scaled changes, potentially underestimating erosion rates. Future studies could integrate higher-resolution datasets (e.g., UAV or LiDAR) and extend the temporal coverage to refine the trend analyses. Additionally, incorporating ecological variables (e.g., coral health, sediment composition) would elucidate feedback mechanisms between morphology and ecosystem function.

In conclusion, this study underscores the fragility and dynamism of coral reef systems in the South China Sea. By disentangling natural and anthropogenic drivers, it provides a scientific foundation for balancing developmental needs with ecological preservation, ensuring the sustainable future of these vital marine ecosystems.

6. Conclusions

This study is primarily based on Landsat, SPOT, and Sentinel-2 satellite remote-sensing images from four different years between 2007 and 2022 as data sources. Quantitative comparative analyses were conducted on the shoreline length, island area, and centroid migration distance of 12 islands and reefs in the Xisha and Nansha archipelagos over nearly 15 years using ENVI and ArcGIS. The DSAS extension module was employed to analyze and explore the temporal and spatial characteristics of shoreline changes on these islands. The main conclusions are as follows:

(1) In the analysis of shoreline and area changes in the 12 coral islands and reefs in Xisha, it was found that the changes in the islands and reefs were influenced by both natural erosion and human intervention. Yongxing Island, as an artificial island, experienced a reduction of 895.65 m in shoreline over 15 years, but its area significantly increased by 982,611.85 m^2. Yagong Island, on the other hand, has continuously suffered from

erosion. Furthermore, although the shoreline of Duncan Island and Yongxing Island was shortened, their areas significantly increased, which may be related to sand accumulation or artificial land reclamation. While the shoreline of North Island increased by 300 m, its area decreased by nearly 5000 m^2, which could be associated with environmental changes or human activities.

(2) In the analysis of shoreline and area changes in the 12 coral islands and reefs in Nansha, it was found that the shoreline changes in most islands and reefs varied greatly from 2007 to 2022. The shorelines of Flat Island, Nanshan Island, and Loaita Island slightly decreased, while Sandy Cay, Namyit Island, and Spratly Island experienced significant growth in both shoreline and area, with Namyit Island's area increasing by 353,619.06 m^2. West York Island saw an increase in shoreline but a decrease in area, indicating that changes in shoreline and area do not always occur synchronously. Between 2012 and 2017, the most significant changes in area occurred on Spratly Island and Northeast Cay.

(3) The most significant changes in the centroids of the Xisha coral islands and reefs occurred between 2012 and 2017, with several islands experiencing considerable centroid migration, particularly Yongxing Island, where the CSR reached 27.40 m/year. From 2017 to 2022, the changes tended to stabilize. In contrast, the Nansha coral islands and reefs experienced smaller changes from 2007 to 2012, with only Southwest Cay showing a noticeable centroid migration. Between 2012 and 2017, a few islands, such as Sin Cowe Island and Spratly Island, exhibited more significant centroid migration, while from 2017 to 2022, the most notable changes were observed on Namyit Island and Sandy Cay. Overall, the Xisha and Nansha coral islands and reefs displayed different trends in their changes.

(4) In the Xisha coral islands and reefs, North Island, Drummond Island, Coral Island, and Yagong Island are in an erosion state, with Drummond Island being particularly affected, as approximately 89% of its shoreline is eroded. Duncan Island, Treasure Island, and South Island show growth, with Yongxing Island exhibiting the most significant increase. In the Nansha coral islands and reefs, Southwest Cay, West York Island, and Zhongye Island are also experiencing erosion, with Spratly Island being the most severely affected. Sandy Cay and Namyit Island show significant growth, with Namyit Island having the highest growth rate. Overall, the Nansha coral islands and reefs predominantly exhibit a trend of expansion.

Author Contributions: Methodology, W.W., P.Z., B.Z. and F.S.; Writing—original draft, F.L. All authors have read and agreed to the published version of the manuscript.

Funding: Strategic Priority Research Program of the Chinese Academy of Sciences, Grant/Award Number: XDB0740300; National Natural Science Foundation of China, Grant/Award Number: 42006171; National Key Research and Development Program of China, Grant/Award Number: 2022YFC3103100 and 2022YFC3103105.

Data Availability Statement: Data is contained within the article.

Conflicts of Interest: The authors declare no conflict of interest.

References

1. Fox, M.D.; Williams, G.J.; Johnson, M.D.; Radice, V.Z.; Zgliczynski, B.J.; Kelly, E.L.; Rohwer, F.L.; Sandin, S.A.; Smith, J.E. Gradients in primary production predict trophic strategies of mixotrophic corals across spatial scales. *Curr. Biol.* **2018**, *28*, 3355–3363.e4. [CrossRef] [PubMed]
2. Anthony, K.R.N.; Kline, D.I.; Diaz-Pulido, G.; Dove, S.; Hoegh-Guldberg, O. Ocean acidification causes bleaching and productivity loss in coral reef builders. *Proc. Natl. Acad. Sci. USA* **2008**, *105*, 17442–17446. [CrossRef] [PubMed]
3. Steers, J.; Stoddart, D. The origin of fringing reefs, barrier reefs and atolls. In *Biology and Geology of Coral Reefs*; Jones, O.A., Endean, R., Eds.; Academic: New York, NY, USA, 1977; pp. 21–57.

4. Talia, M. Sea Level Rise and Implications for Low-Lying Islands, Coasts and Communities, written by Michael Oppenheimer and Bruce C. Glavovic. *Int. J. Public Theol.* **2021**, *15*, 595–597. [CrossRef]
5. Pandolfi, J.M.; Connolly, S.; Marshall, D.; Cohen, A.L. Projecting coral reef futures under global warming and ocean acidification. *Science* **2011**, *333*, 418–422. [CrossRef]
6. Intergovernmental Panel on Climate Change. *Climate Change 2007: The Physical Science Basis*; Intergovernmental Panel on Climate Change: Geneva, Switzerland, 2007; Volume 6.
7. Hopley, D.; Smithers, S.G.; Parnell, K. *The Geomorphology of the Great Barrier Reef: Development, Diversity and Change*; Cambridge University Press: Cambridge, UK; New York, NY, USA, 2007.
8. Spencer, T.; Spalding, M.D. 40224 Coral Reefs of Southeast Asia: Controls, Patterns, and Human Impacts. In *The Physical Geography of Southeast Asia*; Oxford University Press: Oxford, UK, 2005; pp. 402–427.
9. Kleypas, J.A.; Buddemeier, R.W.; Archer, D.; Gattuso, J.-P.; Langdon, C.; Opdyke, B.N. Geochemical consequences of increased atmospheric carbon dioxide on coral reefs. *Science* **1999**, *284*, 118–120. [CrossRef]
10. Ferrario, F.; Beck, M.W.; Storlazzi, C.D.; Micheli, F.; Shepard, C.C.; Airoldi, L. The effectiveness of coral reefs for coastal hazard risk reduction and adaptation. *Nat. Commun.* **2014**, *5*, 3794. [CrossRef]
11. Hughes, T.P.; Barnes, M.L.; Bellwood, D.R.; Cinner, J.E.; Cumming, G.S.; Jackson, J.B.C.; Kleypas, J.; van de Leemput, I.; Morrison, T.H.; Palumbi, S.R.; et al. Coral reefs in the Anthropocene. *Nature* **2017**, *546*, 82–90. [CrossRef]
12. Spalding, M.; Ravilious, C.; Green, E.P. *World Atlas of Coral Reefs*; University of California Press: Berkeley, CA, USA, 2001.
13. Hoegh-Guldberg, O. The Impact of Climate Change on Coral Reef Ecosystems. In *Coral Reefs: An Ecosystem in Transition*; Springer: Dordrecht, The Netherlands, 2011; pp. 391–403.
14. Mumby, P.J.; Skirving, W.; Strong, A.E.; Hardy, J.T.; LeDrew, E.F.; Hochberg, E.J.; Stumpf, R.P.; David, L.T. Remote sensing of coral reefs and their physical environment. *Mar. Pollut. Bull.* **2004**, *48*, 219–228. [CrossRef]
15. Andréfouët, S.; Hochberg, E.J.; Chevillon, C.; Muller-Karger, F.E.; Brock, J.C.; Hu, C. Multi-scale remote sensing of coral reefs. In *Remote Sensing of Coastal Aquatic Environments. Remote Sensing and Digital Image Processing*; Miller, R.L., Del Castillo, C.E., Mckee, B.A., Eds.; Springer: Dordrecht, The Netherlands, 2005; Volume 7, pp. 297–315.
16. Spalding, M.D.; Grenfell, A.M. New estimates of global and regional coral reef areas. *Coral Reefs* **1997**, *16*, 225–230. [CrossRef]
17. Klemas, V. Remote sensing of coastal and ocean currents: An overview. *J. Coast. Res.* **2012**, *28*, 576–586.
18. Zhou, S.; Shi, Q.; Guo, H.; Yang, H.; Yan, H. Evolution of coral shingle cays in the Nansha Islands during 2009–2017. *Trop. Geogr.* **2020**, *40*, 694–708.
19. Roelfsema, C.; Phinn, S.; Udy, N.; Maxwell, P. An integrated field and remote sensing approach for mapping seagrass cover, Moreton Bay, Australia. *J. Spat. Sci.* **2009**, *54*, 45–62. [CrossRef]
20. Genz, A.S.; Fletcher, C.H.; Dunn, R.A.; Frazer, L.N.; Rooney, J.J. The predictive accuracy of shoreline change rate methods and alongshore beach variation on Maui, Hawaii. *J. Coast. Res.* **2007**, *23*, 87–105. [CrossRef]
21. Hapke, C.J.; Himmelstoss, E.A.; Kratzmann, M.G.; List, J.H.; Thieler, E.R. *National Assessment of Shoreline Change: Historical Shoreline Change Along the New England and Mid-Atlantic Coasts*; USA Geological Survey: Reston, VA, USA, 2010.
22. Bhuyan, N.; Sharma, Y.; Sajjad, H.; Ahmed, R. Estimating bank-line migration of the Brahmaputra River in the Middle Brahmaputra floodplains of Assam, India using digital shoreline analysis system. *Environ. Earth Sci.* **2023**, *82*, 385. [CrossRef]
23. Nassar, K.; Mahmod, W.E.; Fath, H.; Masria, A.; Nadaoka, K.; Negm, A. Shoreline change detection using DSAS technique: Case of North Sinai coast, Egypt. *Mar. Georesources Geotechnol.* **2019**, *37*, 81–95. [CrossRef]
24. Sengupta, M.; Ford, M.R.; Kench, P.S.; Perry, G.L.W. Drivers of shoreline change on Pacific coral reef islands: Linking island change to processes. *Reg. Environ. Change* **2023**, *23*, 110. [CrossRef]
25. Shi, J.; Li, C.; Wang, T.; Zhao, J.; Liu, Y.; Xiao, Y. Distribution pattern of coral reef fishes in China. *Sustainability* **2022**, *14*, 15107. [CrossRef]
26. Li, T.; Feng, J.; Zhao, L.; Wang, D.; Fan, R. Geographical distribution of coral reefs and their responses to environmental factors in the South China Sea. *Ecol. Indic.* **2024**, *158*, 111485. [CrossRef]
27. Dai, C.F. Dong-sha Atoll in the South China Sea: Past, present and future. In Proceedings of the Islands of the World VIII International Conference, Kinmen Island, Taiwan, 1–7 November 2004.
28. Liu, L. The fishermen inhabiting the Xuande and Yongle Islands in Xisha Islands. *Int. J. Anthropol. Ethnol.* **2021**, *5*, 10. [CrossRef]
29. Jiang, H.; Su, F.; Zhou, C.; Yang, X.; Wang, Q.; Cheng, F. The geographical characteristics of Nansha Islands in the South China Sea. *J. Geogr. Sci.* **2018**, *28*, 957–972. [CrossRef]
30. Hossain, S.K.A. Assessing the potential effects of climate change on the morphodynamics of the tropical coral reef islands in the Gulf of Mannar, Indian Ocean. *J. Environ. Manag.* **2025**, *375*, 124122. [CrossRef] [PubMed]
31. Dawson, J.L. Multi-decadal shoreline morphodynamics of a shelf-edge reef island, Great Barrier Reef: Implications for future island persistence. *Geomorphology* **2021**, *392*, 107920. [CrossRef]
32. Goble, B.J.; MacKay, F. Cumulative Natural and Human Impacts Alter Cyclical Dynamics of a South African Shoreline: An Extended Summary. *J. Coast. Res.* **2025**, *113*, 289–293. [CrossRef]

33. Duvat, V.K.E.; Magnan, A.K. Rapid human-driven undermining of atoll island capacity to adjust to ocean climate-related pressures. *Sci. Rep.* **2019**, *9*, 15129.
34. Kench, P.S. Effects of Environmental and Climatic Changes on Coral Reef Islands. *Annu. Rev. Mar. Sci.* **2025**, *17*, 301–324. [CrossRef]

Disclaimer/Publisher's Note: The statements, opinions and data contained in all publications are solely those of the individual author(s) and contributor(s) and not of MDPI and/or the editor(s). MDPI and/or the editor(s) disclaim responsibility for any injury to people or property resulting from any ideas, methods, instructions or products referred to in the content.